TESTING, NUMERICAL ANALYSIS AND DESIGN OF HIGH STRENGTH STEEL RHS X-JOINTS

XIAOYI LAN

Department of Civil and Environmental Engineering, The Hong Kong Polytechnic University, Hung Hom, Hong Kong, China
xiaoyi.lan@connect.polyu.hk

This study aims to investigate the structural behaviour of high strength steel (HSS) rectangular hollow section (RHS) X-joints under axial compression in the braces. Eight fabricated RHS X-joints with a measured yield stress of 907 MPa were tested. Finite element (FE) analysis on the RHS X-joints using S460, S690 and S960 steel was conducted. The effects of material strength reduction in the HAZ on the joint strength can be pronounced. The CIDECT strength predictions are generally unconservative for chord face plastification and conservative for chord side wall failure and the combined failure modes of the two. The suggested ranges of brace to chord width ratio (β) and chord width to wall thickness ratio (2γ) are $0.4\leq\beta\leq0.85$ and $2\gamma\leq60\beta$-1 for chord face plastification to allow for more effective use of HSS, and corresponding strength equations were proposed. An analytical model of plate buckling was proposed, and the continuous strength method (CSM) was adopted for the design of chord side wall failure in the RHS X-joints with β=1.0 and 2γ up to 50. The proposed design method is applicable for carbon steel and stainless steel RHS X-joints. The CIDECT linear interpolation approach is suitable for the RHS X-joints with $0.85<\beta<1.0$ and $2\gamma\leq50$ which failed by the combined failure modes. The proposed design rules can produce slightly conservative and consistent strength prediction for the RHS X-joints.

Keywords: high strength steel, RHS X-joints, structural design, static strength

1 Introduction

High strength steel (HSS) with nominal yield stresses higher than 450 MPa is increasingly popular in the infrastructure sector. The application of HSS in tubular structures can lower construction costs and reduce carbon footprints. Design guidance for HSS tubular joints is needed to facilitate applications of HSS tubular structures. Design rules for normal strength steel tubular joints are specified in current design codes and guides. EN 1993-1-8 (CEN 2005) allows for the use of steel grades greater than S355, but stipulates a reduction factor of joint strength of 0.9 for tubular joints in steel grades greater than S355 and up to S460. EN 1993-1-12 (CEN 2007) further extends the material limitation to S700 and imposes a reduction factor of 0.8 for steel grades higher than S460 and up to S700. Likewise, the CIDECT design guide (Packer et al. 2009) also requires the application of a reduction factor of 0.9 combined with the limitation of the yield stress to 0.8 times the ultimate stress. However, the suitability of such design rules for all HSS tubular joints regardless of failure modes remains controversial (Lan and Chan 2019). Investigations are needed to re-evaluate the design rules for HSS tubular joints.

2 Experimental Investigation

Proceedings of the 17th International Symposium on Tubular Structures.
Editors: X.D. Qian and Y.S. Choo

Published by Research Publishing, Singapore.
ISBN: 978-981-11-0745-0; doi:10.3850/978-981-11-0745-0_020-cd

Eight fabricated X-joint specimens as shown in Figure 1 were tested under axial compression in the braces and without restricting the chord ends. Table 1 summarizes the measured dimensions of test specimens. All the steel tubes were fabricated from one QT steel plate with measured thickness of 6.14 mm (i.e. t_0=t_1=6.14 mm, see Figure 1). The measured elastic modulus (E), static yield stress (f_y), static ultimate stress (f_u) and ultimate strain at static ultimate stress (ε_u) are 207 GPa, 907 MPa, 1016 MPa and 5.1%, respectively. Gas metal arc welding (GMAW) was performed using a robotic arm. The current, voltage and welding speed were 150A, 16V and 300 mm/min, and the estimated heat input is 0.38 kJ/mm. The eight test specimens failed by chord face plastification. The static joint strength of RHS X-joints in this study was taken as the ultimate load or the load at an indentation limit of 3%b_0 at the crown, whichever occurred earlier (Packer et al. 2009). The obtained test strengths (N_{Test}) are shown in Table 1.

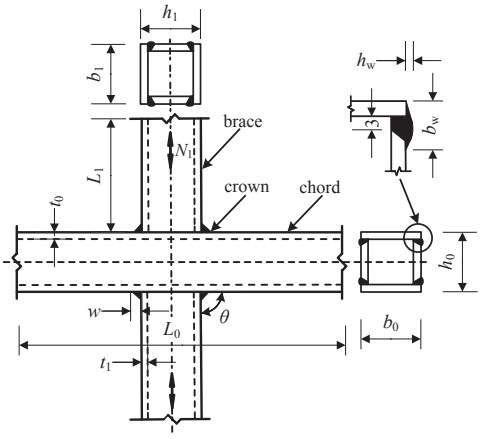

Figure 1. Configuration and notations of fabricated RHS X-joints (dimensions in mm).

Table 1. Measured dimensions of fabricated HSS RHS X-joint specimens.

Specimen	b_0 (mm)	h_0 (mm)	L_0 (mm)	b_1 (mm)	h_1 (mm)	L_1 (mm)	θ (°)	w (mm)	N_{Test} (kN)	N_{FE}/N_{Test}
X1	122.0	122.9	718	96.5	98.3	276	90	7.7	891	0.93
X1#	122.2	122.3	719	96.3	96.1	279	90	7.4	882	0.91
X2	123.0	123.1	719	80.9	81.7	233	90	7.8	541	0.95
X3	122.1	123.3	718	61.3	62.3	171	90	8.2	312	0.97
X3#	121.7	122.8	719	61.5	62.8	172	90	8.7	311	1.02
X4	181.9	182.4	1080	91.1	92.0	260	90	7.1	256	0.84
X5	240.3	242.5	1441	120.4	121.4	351	90	7.2	199	0.89
X6	301.7	301.7	1801	151.3	151.6	439	90	6.7	172	0.93

Note: # denotes repeated tests.

3 Finite Element Analysis

3.1 *Finite element model*

ABAQUS (2013) was used to conduct FE analysis. A FE model using solid elements was developed. The measured dimensions and material properties were employed. The Poisson's ratio (v) was taken as 0.3. Suitable mesh sizes ranging from 5 to 12 mm which depend on the cross-section sizes were adopted for the brace, chord and butt welds, and a mesh size of 3 mm was taken for the fillet welds. One brace end was fixed and all degrees of freedom at the other brace end were restrained except for the brace axial displacement, and the degrees of freedom at

the two chord ends were not restricted, in accordance with the test set-up. Table 1 shows that the developed FE model can produce reasonably accurate prediction of the joint strength.

3.2 *Effects of heat affected zones*

Material properties of heat affected zones (HAZ) mainly depend on the steel material (e.g. TMCP or QT steel), heat input, welding type (e.g. GMAW or laser welding) and cooling time (Lan et al. 2018a). The strength reduction in the HAZ could be significant for HSS if welding parameters are not properly controlled. It is thus necessary to examine effects of HAZ on the joint strength. FE analysis was conducted on the RHS X-joints using S960 steel (see Table 2). Figure 2 shows the adopted HAZ dimensions, and the material strength reduction in red and blue regions are 20% and 10%, respectively, according to Lan et al. (2018a). The material properties and stress-strain curves of S960 steel were taken in line with Ban and Shi (2018). Table 2 shows that effects of material strength reduction in HAZ on the joint strength can be more pronounced for the X-joints with medium β ratio than those with small or large β ratio.

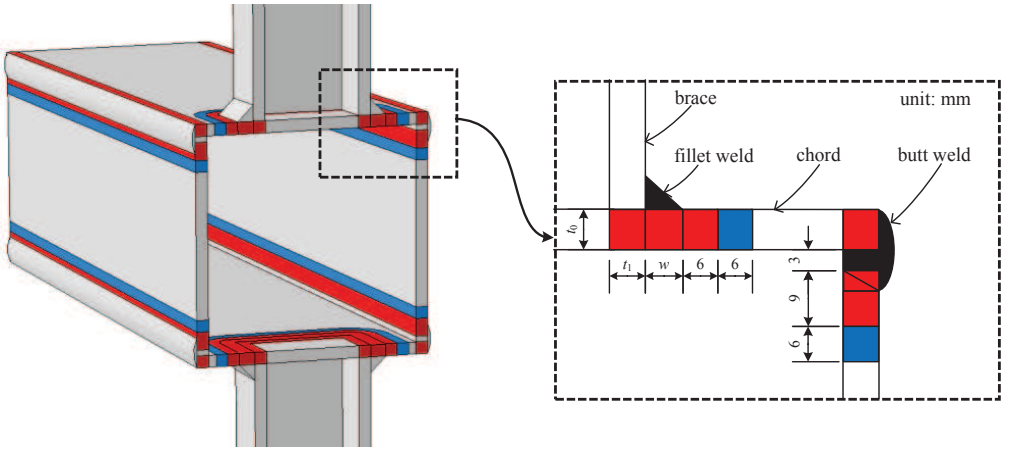

Figure 2. Heat affected zones in S960 steel RHS X-joints.

Table 2. Effects of heat affected zones on fabricated RHS X-joints in S960 steel.

Specimen	b_0 (mm)	h_0 (mm)	h_1 (mm)	t_1 (mm)	β	2γ	N_{u1} (kN)	N_{u2}/N_{u1}
X1	122.0	122.9	98.3	6.14	0.79	19.9	825	0.96
X1-1	122.0	122.9	122.9	6.14	1.00	19.9	1704	0.92
X1-2	122.0	122.9	122.9	2.44	1.00	50.0	272	0.99
X3	122.1	123.3	62.3	6.14	0.50	20.0	303	0.86
X3-1	122.1	123.3	24.7	6.14	0.20	20.0	105	0.92
X6	301.7	301.7	151.6	6.14	0.50	49.1	161	0.85

Note: $\beta=b_1/b_0$ and $2\gamma=b_0/t_0$; N_{u1} and N_{u2} represent the joint strengths without and with HAZ, respectively.

3.3 *Parametric study*

FE analysis on 585 fabricated RHS X-joints in S460, S690 and S960 steel was conducted without modelling the HAZ. Effects of HAZ were considered by proposing conservative strength equations in Section 5. The welds were modelled in line with the minimum requirements for butt welds (AWS 2010). The examined parameter ranges are $0.3\leq\beta\leq1.0$, $10\leq2\gamma\leq50$ and $-0.8\leq n\leq0.8$. The chord preload ratio (n) is the ratio of the chord preload (N_p) to the chord cross-section yield load (Af_y). The material properties and stress-strain curve models of S460, S690 and S960 steel proposed by Ban and Shi (2018) were adopted. The FE model in

Section 3.1 was used. The mesh sizes were determined by a mesh convergence study. The RHS X-joints failing by local buckling of brace or chord will be excluded in the subsequent analysis.

4 Evaluation of CIDECT Design Rules for RHS X-joints

The CIDECT design strength equation for hot-finished and cold-formed normal strength steel RHS X-joints with $\beta \leq 0.85$ which failed by chord face plastification is as follows:

$$N_{\text{CIDECT,Rd}} = \left(\frac{2\eta}{(1-\beta)\sin\theta} + \frac{4}{\sqrt{1-\beta}} \right) Q_{\text{f,CIDECT}} \frac{f_y t_0^2}{\sin\theta} \tag{1}$$

where η is the ratio of brace depth (h_1) to chord width (b_0), β is the ratio of brace width (b_1) to chord width (b_0), θ is the angle between the brace and chord, f_y is the steel yield stress, t_0 is the chord wall thickness, and $Q_{\text{f,CIDECT}}$ is the chord stress equation. Eq. (1) is based on the yield line model and a safety factor of 1.0 is incorporated (Wardenier 1982). The CIDECT design strength equation for the RHS X-joints with β=1.0 failing by chord side wall failure is as follows:

$$N_{\text{CIDECT,Rd}} = \left(\frac{2h_1}{\sin\theta} + 10t_0 \right) Q_{\text{f,CIDECT}} \frac{f_k t_0}{\sin\theta} \tag{2}$$

where f_k is the column buckling stress. Eq. (2) is based on the stub column buckling model and a safety factor of 1.25 is built-in (Wardenier 1982). A linear interpolation between the above two cases is stipulated for $0.85<\beta<1.0$. It is noted that the validity ranges of the CIDECT strength equations are $(0.1+0.02\gamma) \leq \beta \leq 1.0$ with a minimum β value of 0.25 and $2\gamma \leq 40$, and the cross-section should be class 1 or 2 for the chord under compression. The CIDECT strength prediction (N_{CIDECT}) was derived by setting the built-in safety factors to be unity, and then compared with the obtained test and FE strengths (N_{Test} and N_{FE}) as shown in Figure 3. The $N_{\text{CIDECT}}/N_{\text{FE}}$ and $N_{\text{CIDECT}}/N_{\text{Test}}$ ratios generally increase with decreasing β ratio and with increasing 2γ ratio and steel grade for $\beta \leq 0.85$. The $N_{\text{CIDECT}}/N_{\text{FE}}$ ratio generally increases with decreasing 2γ ratio, and the effects of β ratio and steel grade on the $N_{\text{CIDECT}}/N_{\text{FE}}$ ratio are relatively minor for $0.85<\beta \leq 1.0$. Table 3 show that the CIDECT strength prediction is unconservative and scattered for the RHS X-joints with $0.3 \leq \beta \leq 0.85$, and conservative for $0.85<\beta<1.0$. The CIDECT strength prediction is unduly conservative and scattered for β=1.0. Table 4 shows that the CIDECT prediction of joint strength reduction ($Q_{\text{f,CIDECT}}$) is conservative and relatively scattered.

Table 3. Results of statistical analysis for fabricated HSS RHS X-joints without chord preload.

Parameter	$N_{\text{CIDECT}}/N_{\text{FE}}$			$N_{\text{Proposed}}/N_{\text{FE}}$		
	No. of data	Mean	COV	No. of data	Mean	COV
$0.3 \leq \beta \leq 0.85$	162	1.23	0.333	84	0.85	0.134
$0.85<\beta<1.0$	27	0.68	0.154	27	0.91	0.072
β=1.0	105	0.52	0.525	105	0.92	0.076
Total	294	0.93	0.522	216	0.89	0.107

Table 4. Results of statistical analysis for fabricated HSS RHS X-joints with chord preload.

Parameter	$Q_{\text{f,CIDECT}}/Q_{\text{f,FE}}$			$Q_{\text{f,Proposed}}/Q_{\text{f,FE}}$		
	No. of data	Mean	COV	No. of data	Mean	COV
S460	72	0.96	0.099	50	0.97	0.067
S690	72	0.94	0.099	50	0.96	0.069

S960	72	0.93	0.112	50	0.95	0.084
Total	216	0.94	0.103	150	0.96	0.074

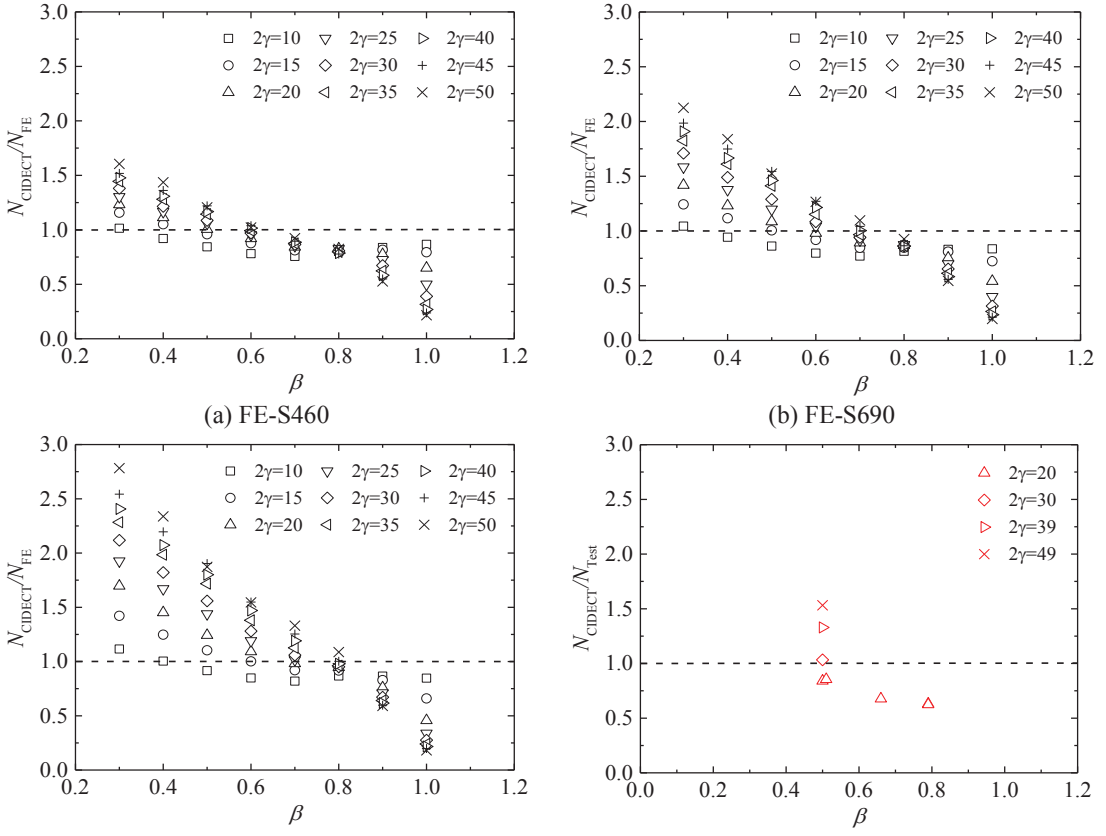

(a) FE-S460 (b) FE-S690

(c) FE-S960 (d) Tests (f_y=907 MPa)

Figure 3. Comparison of joint strengths for fabricated RHS X-joints without chord preload.

5 Proposed Design Rules for HSS RHS X-joints

5.1 *Chord face plastification*

The CIDECT strength prediction for chord face plastification is unconservative for small β ratio and large 2γ ratio as discussed in Section 4. It is suggested to limit the ranges of β and 2γ ratios to be $0.4 \le \beta \le 0.85$ and $2\gamma \le 60\beta - 1$ in order to allow for more effective use of HSS. The cross-section of chord members should be class 1 or 2 when the chord is under compression to avoid local buckling of chord members. Regression analysis of numerical results obtained in this study was conducted to propose strength equations for the RHS X-joints using steel grades ranging from S460 to S960 which failed by chord face plastification as follows:

$$N_{\mathrm{CIDECT,Rd}} = \left(\frac{2\eta}{(1-\beta)\sin\theta} + \frac{4}{\sqrt{1-\beta}} \right) Q_{\mathrm{y}} Q_{\mathrm{f,Proposed}} \frac{f_{\mathrm{y}} t_0^2}{\sin\theta} \tag{3}$$

$$Q_{\mathrm{y}} = -62 f_{\mathrm{y}} / E + 1.1 \tag{4}$$

$$Q_{\mathrm{f,Proposed}} = (1 - |n|)^{C_{\mathrm{P}}} \tag{5}$$

$$C_P = \begin{cases} 0.50 - 0.45\beta & \text{for n<0} \\ 0.15 & \text{for n} \geq 0 \end{cases} \quad (6)$$

where Q_y is the proposed reduction factor of joint strength and $Q_{f,Proposed}$ is the proposed chord stress function in which n is the chord preload ratio. Negative and positive values of n denote compressive and tensile chord preloads, respectively. The joint strengths calculated from the proposed strength equations ($N_{Proposed}$) were compared with the FE strengths (N_{FE}) for the RHS X-joints without chord preload. Table 3 shows that the proposed strength equations can produce somewhat conservative and less scattered strength prediction. The proposed strength equations are conservative in order to consider the joint strength reduction resulted from the HAZ which could be up to 15% for chord face plastification as discussed in Section 3.2. Table 4 shows that the proposed chord stress equation is reasonably accurate and slightly conservative.

5.2 *Chord side wall failure*

The CIDECT strength prediction is unduly conservative and scattered for the RHS X-joints with β=1.0 which failed by chord side wall failure as discussed in Section 4. An analytical model of plate buckling which could consider the beneficial restraints of chord faces and braces for the chord side walls was proposed. The continuous strength method (CSM) originally developed for designing non-slender stainless steel cross-sections by Gardner and Nethercot (2004) was also adopted to exploit the beneficial effect of strain hardening in non-slender chord side walls. Figure 4 shows the proposed analytical model for the chord side wall failure in RHS X-joints. The chord side wall is idealized as a plate under localized stresses (p) from the braces over the intersecting width of $h_1/\sin\theta$ and with plate length of L_0, height of h_0 and thickness of t_0.

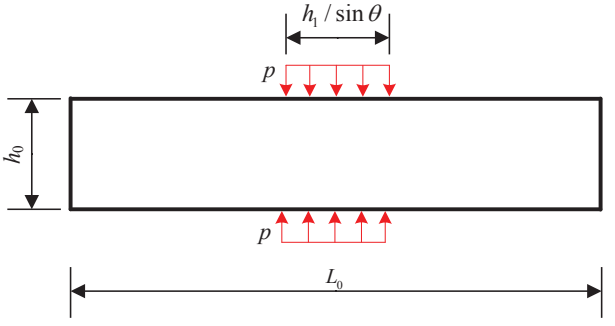

Figure 4. Proposed analytical model for chord side wall failure in RHS X-joints.

In order to obtain the elastic buckling stresses (f_{cr}) of the chord side walls which incorporate the restraint effects of the chord faces and the braces, elastic eigenvalue analysis on the RHS X-joints was conducted using the developed FE model in Section 3.1. Regression analysis of the obtained elastic buckling stresses ($f_{cr,FE}$) was conducted to derive the function of f_{cr} as follows:

$$f_{cr,Proposed} = 3.2\frac{\pi^2 E}{12(1-\nu^2)}\left(\frac{t_0}{h_e}\right)^{1.96}\left(\frac{h_0}{h_1/\sin\theta}\right)^{0.66} \quad (7)$$

where h_e is the effective buckling length which is taken as h_0-2t_0 for the fabricated RHS X-joints and h_0 for cold-formed and hot-finished steel RHS X-joints to consider the shape effect of chord corners (sharp or round). The CSM was adopted to consider strain hardening for chord side wall failure in RHS X-joints. The FE results of the fabricated RHS X-joints obtained in Section 3.3

and test results in the literature were used to develop the CSM. The test results include those of RHS X-joints using hot-finished and cold-formed carbon steel (Packer 1984, Chen and Becque 2016, Pandey and Young 2017) and cold-formed stainless steel (Feng and Young 2011). The cross-section slenderness (λ_p) of chord side walls is defined as $(f_y/f_{cr})^{1/2}$. The base curves were proposed for the chord side walls using regression analysis of the obtained FE results as follows:

$$\frac{\varepsilon_{csm}}{\varepsilon_y} = \frac{0.50}{\lambda_p^{1.80}} \le \min\left(15, \frac{C_1\varepsilon_u}{\varepsilon_y}\right) \quad \text{for } \lambda_p \le 0.68 \tag{8}$$

$$\frac{\varepsilon_{csm}}{\varepsilon_y} = 0.91\left(1 - \frac{0.22}{\lambda_p^{1.60}}\right)\frac{1}{\lambda_p^{1.60}} \quad \text{for } 0.68 < \lambda_p \le 1.78 \tag{9}$$

where ε_{csm} is the CSM limiting strain, ε_y is the yield strain. Two upper limits ($15\varepsilon_y$ and $C_1\varepsilon_u$) are imposed to the ε_{csm} (see Eq. (8)) to avoid excessive plastic strain and material fracture for non-slender cross-sections (Gardner and Nethercot 2004). Values of the coefficient (C_1) reported by Buchanan et al. (2016) for various steel materials were adopted.

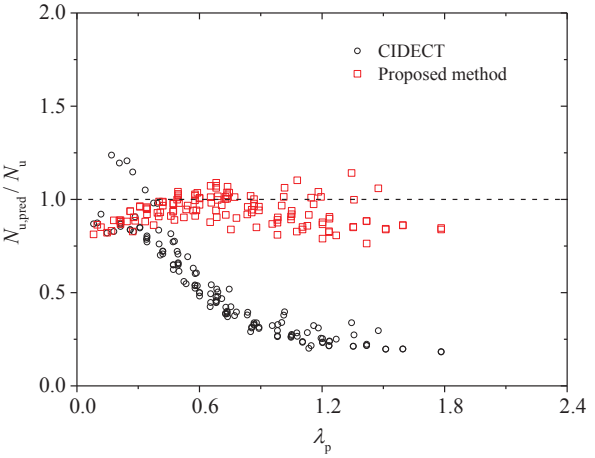

Figure 5. Comparison of FE and test strengths of equal-width RHS X-joints with predicted strengths.

The CSM elastic, linear hardening material models adopted by Lan et al. (2018b) were also employed to obtain the CSM limiting stress (f_{csm}) for the chord side wall failure in the RHS X-joints. The static strength of the chord side wall failure in the equal-width RHS X-joints under brace axial compression ($N_{Proposed}$) can be determined from:

$$N_{Proposed} = \frac{f_{csm}t_0}{\sin\theta}\left(2h_1 + a_1t_0\right)Q_{f,Proposed} \quad \text{for } \lambda_p \le 0.68 \tag{10}$$

$$N_{Proposed} = \frac{\varepsilon_{csm}}{\varepsilon_y}\frac{f_yt_0}{\sin\theta}\left(2h_1 + a_2t_0\right)Q_{f,Proposed} \quad \text{for } 0.68 < \lambda_p \le 1.78 \tag{11}$$

Regression analysis of the FE and test results was conducted to derive the coefficients of a_1 and a_2. It is suggested that a_1=a_2=8 for the fabricated RHS X-joints with sharp chord corners, and a_1=6 and a_2=0 for the hot-finished and cold-formed RHS X-joints with round chord corners. Table 3 shows that the proposed design method herein can produce slightly conservative and

consistent strength prediction. The conservative strength equations were proposed to consider the joint strength reduction resulted from the HAZ which could be up to 8% for the RHS X-joints failing by chord side wall failure as discussed in Section 3.2. Figure 5 shows that the proposed design method can produce much more accurate and consistent strength prediction than the CIDECT design guide (Packer et al. 2009).

5.3 *Combined failure modes*

The proposed strength equations for $\beta \leq 0.85$ and those with $\beta=1.0$ can provide accurate and consistent strength predictions as discussed in Sections 5.1 and 5.2, and thus the CIDECT linear interpolation approach is suggested for $0.85<\beta<1.0$. Table 3 shows that the linear interpolation can produce slightly conservative and consistent strength prediction.

6 Conclusions

The structural behaviour of fabricated RHS X-joints using steel grades ranging from S460 to S960 and under axial compression in the braces was examined. The joint strength reduction resulted from the material strength reduction in the HAZ can be more significant for medium β ratio than small or large β ratio. The CIDECT strength prediction is unconservative for chord face plastification, and conservative for chord side wall failure and the combined failure modes of the two. The suggested ranges of β and 2γ are $0.4 \leq \beta \leq 0.85$ and $2\gamma \leq 60\beta$-1 for chord face plastification to allow for more effective use of HSS, and corresponding strength equations were proposed. An accurate design method was proposed for chord side wall failure. The proposed design method is applicable for carbon steel and stainless steel RHS X-joints. The CIDECT linear interpolation approach is suitable for the combined failure modes. The proposed strength equations can produce much more accurate and consistent strength prediction than the current CIDECT design rules.

References

ABAQUS, Version 6.13-1, USA: K. a. S. Hibbit, 2013.

AWS, Structural welding code-steel, USA: AWS D1.1/D1.1M, 2010.

Ban, H. and Shi, G., Overall buckling behaviour and design of high-strength steel welded section columns, *J. Constr. Steel Res.*, 143, 180-195, 2018.

Buchanan, C., Gardner, L. and Liew, A., The continuous strength method for the design of circular hollow sections, *J. Constr. Steel Res.*, 118, 207-216, 2016.

CEN, Eurocode 3, Design of steel structures-Part 1-8: Design of joints, EN 1993-1-8, Brussels, 2005.

CEN, Eurocode 3: Design of steel structures-Part 1-12: Additional rules for the extension of EN 1993 up to steel grades S700, EN 1993-1-12, Brussels, 2007.

Cheng, S. and Becque, J., A design method for side wall failure of RHS truss X-joints accounting for compressive chord pre-load, *Eng. Struct.*, 126, 689-702, 2016.

Feng, R. and Young, B., Design of cold-formed stainless steel tubular T-and X-joints, *J. Constr. Steel Res.*, 67(3), 421-436, 2011.

Gardner, L. and Nethercot, D., Structural stainless steel design: a new approach, *Struct. Eng.*, 82,2-28, 2004.

Lan, X.Y., Chan, T.M. and Young, B., Structural behaviour and design of chord plastification in high strength steel CHS X-joints, *Constr. Build. Mater.*, 191, 1252-1267, 2018a.

Lan, X.Y., Chen, J.B., Chan, T.M. and Young, B., The continuous strength method for the design of high strength steel tubular sections in compression, *Eng. Struct.*, 162, 177-187, 2018b.

Lan, X.Y. and Chan, T.M., Recent research advances of high strength steel welded hollow section joints, *Struct.*, 17, 58-65, 2019.

Packer, J.A., Web crippling of rectangular hollow sections, *J. Struct. Eng.*, 110(10), 2357-2373, 1984.

Packer, J.A., Wardenier, J., Zhao, X.L., van der Vegte, G.J. and Kurobane, Y., Design guide for rectangular hollow section (RHS) joints under predominantly static loading, CIDECT, Germany, 2009.